



The Open Civil Engineering Journal

Content list available at: <https://opencivilengineeringjournal.com>



RESEARCH ARTICLE

Behavior of Fibrous Reinforced Concrete Splices

Mereen H.F. Rasheed¹, Ayad Z.S. Agha^{1,*} and Bahman O. Taha¹

¹Department of Civil Engineering, Erbil Technical Engineering College, Erbil Polytechnic University., Erbil, Iraq

Abstract:

Background:

The tangent of the relationship between bond stress and displacement (slip) is called the modulus of displacement and gives the basis for the theory. This theory is used to determine the stress distribution along the spliced reinforcement bars.

Objective:

This research presents a modification on the theory of the modulus of displacement to determine the stress distribution along the spliced reinforcement bond for fibrous reinforced concrete.

Methods:

- 1- General differential equations are derived for concrete stress, stress in reinforcement bars and bond stress between reinforcement bars and surrounding concrete.
- 2-The general solutions of these D.E. are determined and Excel data sheets are prepared to apply these solutions and determine the concrete, steel and bond stresses.

Results:

Excel data sheets are prepared to determine the concrete, steel and bond stresses. The stresses are determined along the bar splice length considering the effect of steel fiber content.

Conclusion:

The maximum concrete stress is obtained at center $x=0$ and minimum at $(x = \mp \frac{L}{2})$. Maximum bond stress obtained at $(x = \mp \frac{L}{2})$ and minimum at the center. The maximum steel stress at $(x = -\frac{L}{2})$ and minimum at $(x = \frac{L}{2})$. The value of (σ_{\max}) increased linearly with increasing of (ρ) . The concrete stress increased nonlinearly with $(\rho\%)$ and linearly with (F_y) and (f_c') . Also increasing of (k) and bar diameter have small effects. The value of bond stress decreased linearly with (Qf) and $(\rho\%)$.

Keywords: Bond stress, Fibrous concrete, Concrete, Splices, Volume fraction, Modulus of displacement.

Article History

Received: December 30, 2020

Revised: August 23, 2021

Accepted: September 7, 2021

1. INTRODUCTION

Modulus of displacement theory is used to determine the stress distribution along the spliced reinforcement bars. The tangent of the relationship between bond stress and displacement (slip) is called the modulus of displacement and gives the basis for the theory. Fig. (1) shows the relation between bond stress and displacement (slip).

Losberg investigated the bond properties of long concrete

specimens with pulled, axially embedded reinforcement bars [1]. He used the modulus of displacement theory for the calculation of the stresses and the crack widths. Also, he extended the investigations to the curtailment of reinforcement in accordance with the moment diagram, and the influence of cracks was also studied.

Feldman and Bartlett showed that bond stress magnitude varies along the length of plain reinforcing bars in pullout specimens by using analytical methods and experimental tests [2]. They established analytical relationships between bond stress and slip at the unloaded end of the bar and along the length of the bar. The analytical relationship showed that the

* Address correspondence to this author at Department of Civil Engineering, Erbil Technical Engineering College, Erbil Polytechnic University, Erbil, Iraq; Tel: 009647504454107; E-mail: ayad.saber@epu.edu.iq

bond stress is a function of bar slip, slip is a function of bar force, and bar force is a function of bond stress. Also, they concluded that the maximum load occurs just before slip occurs at the unloaded end of the bar, and the location of the peak bond stress shifts from the loaded end towards the unloaded end of the specimen with increasing applied load.

Thompson *et al.* studied the anchorage behavior of headed reinforcement in lap splices by experimental tests [3]. They concluded that the stress is transferred between opposing bars in non-contact lap splices through struts acting at an angle to the direction of the bar. Anchorage length in non-contact lap splices could be determined by drawing the struts between opposing bars propagate at an angle of 55° with respect to the bar axis.

Coogler *et al.* tested two commercially available offset mechanical splice systems in direct tension with the splice both restrained and unrestrained from rotation [4]. They concluded that pullout failure was the most common failure mode observed. This mode of failure results in a decrease in apparent ultimate stress for the system because of the inability to develop the full strength of the cross-section. A 345 MPa stress range for fatigue testing results in fatigue-induced reinforcing bar rupture at a very low number of cycles. A more reasonable stress range of 138 MPa is suggested for assessing the performance of this type of splice. Also, for all in-place testing, concrete was unable to properly confine the offset splice near ultimate load levels.

Feldman and Bartlett concluded that there is a complicated interaction between flexural and shear behavior, bond stress, and cracking two full-scale T-beams, 4.2m long with $a/d=7.5$ were tested in four-point loading [5]. Both were reinforced with plain hollow steel bars that had roughened surfaces to simulate bars found in historic structures. The flexural reinforcement ratios were 0.33% for the HSS bar and 0.98% for plane bars. Arch action initiated in the beam reinforced with plane bars due to loss of bond in the constant shear region near midspan when the applied load reached 60% of its maximum value. The beam reinforced with the HSS bars had lesser bond demand, and arch action due to bond loss did not initiate in the beam until the maximum load was achieved. Also, when shear is carried by beam action, bond demand is greatest within the elastic-uncracked region adjacent to the first flexural crack.

Yang and Ashour developed a mechanical analysis based on an upper-bound theorem to predict the optimum failure surface and concrete breakout capacity of single anchors under tensile loads [6]. The predicted results obtained from ACI 318-05 are compared with the experimental test results. They concluded that the shape of the failure surface predicted by the mechanism analysis is significantly influenced by the ratio of effective tensile and compressive strengths of concrete. The concrete breakout capacity of anchors predicted from mechanism analysis responds sensitively to the variation of the ratio between effective tensile and compressive strengths of concrete. Conservation of ACI 318-05 sharply increases in specimens having concrete strength above 50 MPa, whereas the mechanism analysis shows good agreement with tests results, regardless of concrete strength.

Sezen and Setzler showed that the contribution of bar slip deformations to total member lateral displacement could be significant [7]. In addition to flexural deformations, bar slip deformations should be considered in the modeling and analysis of reinforced concrete members. They present a method for computing slip for bars stressed, its unloaded end, and hooked bars. The proposed model is compared with five models found in the literature and three independent sets of experimental data. Also, the proposed model is used to calculate the lateral load-slip displacement relations for seven columns from two different studies, and the computed relations compare well with the measured test results.

Howell and Higgins studied the bond performance of square and round deformed reinforcing bars [8]. They concluded that the application of the simplified ACI development length equations to characterize the reinforcing bar stress provided a reasonable lower bound for both square and round bars across all test types. Also, the ACI approach was conservative for partial reinforcing bar embedment of round and square results and indicated that linear interpolation of available reinforcing bar stress for embedment lengths less than the computed development length also appears reasonable for the square reinforcing bar. Computation of development length using the ACI formula with an equivalent round diameter for square reinforcing bar results in lengths (13%) larger than when the side dimension is used. This is conservative and available for large square reinforcing bar sizes and alternative test configurations.

Eligehausen *et al.* proposed a model to predict the average failure load of anchorage using adhesive banded anchors based on numerical and experimental investigations [9]. The model is similarly cast in place, and post-installed mechanical anchors are incorporated in ACI 318-05, but with the following modifications:

- (1) The basic strength of a single adhesive anchor predicts the pullout capacity and not the concrete breakout capacity.
- (2) The critical spacing and critical edge distance of adhesive anchorages depend on the anchor diameter and the bond strength and not on the anchor embedment depth.
- (3) The proposed model results agree very well with the results of (415) group tests contained in a worldwide database.

This research presents a modification on the theory of the modulus of displacement that has been presented by Tepfers [10] to determine the stress distribution along the spliced reinforcement bond for fibrous reinforced concrete.

2. MATERIALS AND METHODS

2.1. Theoretical Analysis

2.1.1. Basic Equations

- 1- The splice area is located in the region of the constant moment and has no shear.
- 2- The stress in the reinforcement at both ends of the splice is equal.
- 3- Moment cracks in the concrete are located at the

ends of the splice, and the stress in the reinforcement is (σ_s). Fig. (2) shows the tension reinforcement splice.

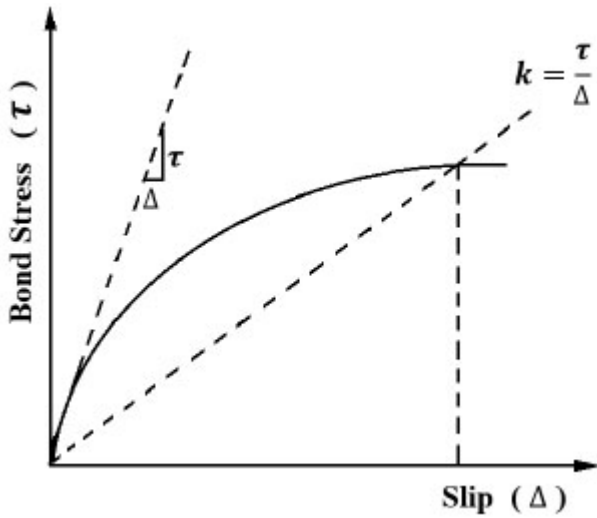


Fig. (1). Bond stress-slip relationship.

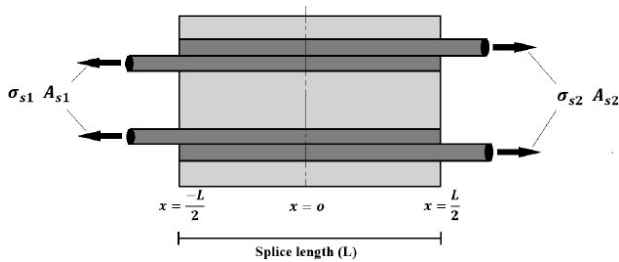


Fig. (2). Tension reinforcement splice.

From Fig. (1); the bond stress between reinforcement and concrete:

$$\tau = k \Delta \tag{1}$$

Where τ = bond stress. (MPa) N/mm²

k = modulus of displacement (N/mm³)

Δ = displacement or slip (mm)

The connection between bond stress (τ) and normal stress of concrete (σ_c) and steel stress (σ_s) shown in Fig. (3):

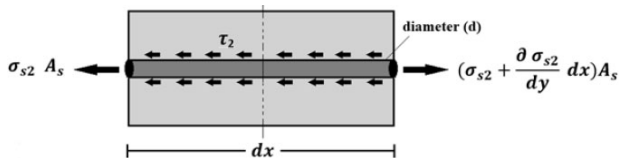


Fig. (3). Equilibrium of splice bar.

The horizontal equilibrium of splice bar at $x = \frac{L}{2}$ gives the following equations:

$$\sum F_x = 0$$

$$\sigma_{s2} A_{s2} + \tau_2 u dx = \left(\sigma_{s2} + \frac{d\sigma_{s2}}{dx} dx \right) A_{s2} \tag{2}$$

$$\tau_2 u dx = \frac{d\sigma_{s2}}{dx} dx A_{s2}$$

$$\frac{d\sigma_{s2}}{dx} = \tau_2 \frac{u}{A_{s2}}$$

Also by the same way:

$$\frac{d\sigma_{s1}}{dx} = \tau_1 \frac{u}{A_{s1}} \tag{3}$$

Where: d = diameter of the bar (mm).

A_s = Cross-sectional area of the bar (mm²)

u = perimeter of the bar (mm)

τ^1 = bond stress at $x = -\frac{L}{2}$ (MPa)

σ_s^1 = tension steel stress at $\frac{L}{2}$ (MPa)

τ^2 = bond stress at $x = \frac{L}{2}$ (MPa)

σ_s^2 = tension stress at $x = -\frac{L}{2}$ (mpa)

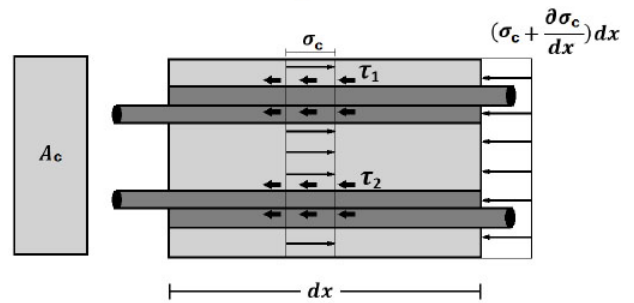


Fig. (4). Equilibrium of steel concrete connection within the splice.

Concrete stress is determined from the horizontal equilibrium of the concrete steel connection shown in Fig. (4);

$$\sigma_c A_c - \tau_1 u dx - \tau_2 u dx - \left(\sigma_c + \frac{d\sigma_c}{dx} \right) dx A_c = 0 \tag{4}$$

$$\frac{d\sigma_c}{dx} = -\frac{u}{A_c} (\tau_1 + \tau_2)$$

Where σ_c = tensile stress in the effective concrete (MPa).

A_c = effective area of the concrete around the steel (mm²).

The equilibrium condition for the splice is shown in Fig. (5)

$$\sigma_c A_c + \sigma_{s1} A_{s1} + \sigma_{s2} A_{s2} = A_s f_s \tag{5}$$

Where: f_s = tension stress of the steel reinforcement (MPa).

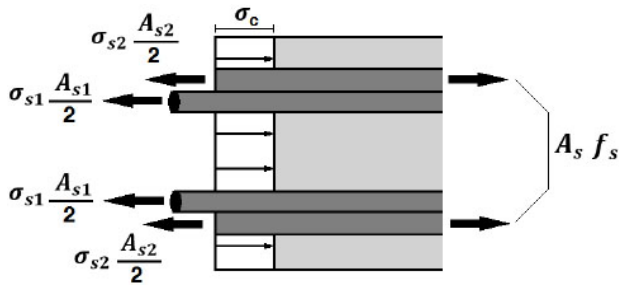


Fig. (5). Equilibrium of the splices.

From Eq.(1); derivate on both sides :

$$\frac{d\tau}{dx} = k \frac{d\Delta}{dx} \tag{6}$$

The strain is the difference in displacement between the two materials, concrete, and steel.

$$\epsilon = \frac{d\Delta}{dx} = \frac{\sigma}{E} \tag{7}$$

The change in shear stress for element length (dx) due to the displacement between the reinforcement bar and the concrete for both parts of the splice is:

$$\frac{d\tau_1}{dx} = k(\epsilon_{s1} - \epsilon_c) \tag{8}$$

Or

$$\frac{d\tau_1}{dx} = k \left(\frac{\sigma_{s1}}{E_s} - \frac{\sigma_c}{E_c} \right) \tag{9}$$

And

$$\frac{d\tau_2}{dx} = k(\epsilon_{s2} - \epsilon_c) \tag{10}$$

Or

$$\frac{d^2\sigma_c}{dx^2} = \frac{-u}{A_c} \left(\frac{d\tau_1}{dx} + \frac{d\tau_2}{dx} \right) \tag{11}$$

Take the derivative of both sides of Eq. (4);

$$\frac{d^2\sigma_c}{dx^2} = \frac{-u}{A_c} \left(\frac{d\tau_1}{dx} + \frac{d\tau_2}{dx} \right) \tag{12}$$

Substitute Eq. (9 and 11) into Eq. (12) to get;

$$\frac{d^2\sigma_c}{dx^2} = \frac{-uk}{A_c} \left(\frac{\sigma_{s2}}{E_s} + \frac{\sigma_{s2}}{E_s} - \frac{2\sigma_c}{E_c} \right) \tag{13}$$

$$\frac{d^2\sigma_c}{dx^2} = \frac{-uk}{A_c E_s} E_s [(\sigma_{s1} + \sigma_{s2}) - 2\sigma_c \frac{E_s}{E_c}] \tag{14}$$

From Eq. (5);

$$\sigma_{s1} + \sigma_{s2} = f_s - \sigma_c \frac{A_c}{A_s} \tag{15}$$

the bar diameter is taken the same at both side of the splice, thus:

$$A_s = A_{s1} = A_{s2}$$

Subacute Eq. (15) into Eq. (14);

$$\frac{d^2\sigma_c}{dx^2} = \frac{-uk}{A_c E_s} \left[f_s - \sigma_c \frac{A_c}{A_s} - 2\sigma_c \frac{E_s}{E_c} \right] \tag{16}$$

taking $\rho =$ reinforcement index $\frac{A_s}{A_c}$

and $n =$ modular ratio $\frac{E_s}{E_c}$

$$\frac{d^2\sigma_c}{dx^2} = \frac{-uk}{A_c E_s} \left[\sigma_s - \sigma_c \left(\frac{1}{\rho} + 2n \right) \right] \tag{17}$$

$$\frac{d^2\sigma_c}{dx^2} = \frac{-uk}{A_c E_s \rho} \left[\sigma_s \rho - \sigma_c (1 + 2n\rho) \right] \tag{18}$$

but $A_c E_s \rho = A_c \frac{A_s}{A_c} E_s = A_s E_s$

re-arrange Eq. (18) to get:

$$\frac{d^2\sigma_c}{dx^2} - \frac{uk}{E_s A_s} (1 + 2n\rho) \sigma_c = \frac{-uk}{E_s A_s} \rho \sigma_s \tag{19}$$

Let $k_1^2 = \frac{uk}{E_s A_s} (1 + 2n\rho)$

$$\frac{d^2\sigma_c}{dx^2} - k_1^2 \sigma_c = \frac{k_1^2 \rho}{1 + 2n\rho} \sigma_s \tag{20}$$

The general solution of Eq. (20) is:

$$\sigma_c = A \sinh k_1 x + B \cosh k_1 x + \frac{\sigma_{s0} \rho}{1 + 2n\rho} \tag{21}$$

The constants A and B are determined by application of the boundary conditions:

at $x = \mp \frac{L}{2}$; $\sigma_c = \sigma f_u$ for fibrous concrete

$\sigma_c = 0$ for concrete without fibers.

The tensile strength of plain concrete with steel fiber can be calculated from the following equations (11, 12).

$$\sigma_f = 0.82\tau F$$

where: $\tau =$ Interfacial bond strength between steel fiber and concrete matrix.

$f =$ Fiber factor (13, 14) = $Q_f \frac{L_f}{D_f}$

$Q_f =$ volume fraction of steel fiber (%).

$d_f =$ Bond factor depends on the type of steel fiber.

$L_f =$ Length of steel fiber (mm).

$D_f =$ Diameter of steel fiber (mm).

These give the constants as:

$$A = 0 \tag{22}$$

$$B = \left(\sigma f_u - \frac{\sigma_s \rho}{1 + 2n\rho} \right) \frac{1}{\cosh \frac{k_1 L}{2}} \tag{23}$$

The final form of the concrete normal stress is:

$$\sigma_c = \left(\sigma f_u - \frac{\sigma_s \rho}{1 + 2n\rho} \right) \frac{\cosh k_1 x}{\cosh \frac{k_1 L}{2}} + \frac{\sigma_s \rho}{1 + 2n\rho} \tag{24}$$

for concrete without steel fiber: $\sigma f_u=0$;

$$\sigma_c = \frac{\sigma_{s0} \rho}{1+2n\rho} \left(1 - \frac{\cosh k_1 x}{\cosh \frac{k_1 L}{2}}\right) \quad (25)$$

The normal stress (σ_{s1}) is determined by derivation of Eq. (3) and combined with Eq. (9) to get:

$$\frac{d^2 \sigma_{s1}}{dx^2} = \frac{u}{A_s} \frac{d\tau_1}{dx} \quad (26)$$

$$\frac{d^2 \sigma_{s1}}{dx^2} = \frac{uk}{A_s} \left[\frac{\sigma_{s1}}{E_s} - \frac{\sigma_c}{E_c}\right] \quad (27)$$

rearrangement of Eq. (27);

$$\frac{d^2 \sigma_{s1}}{dx^2} - \frac{uk}{A_s E_s} \sigma_{s1} = -\frac{uk}{A_s E_s} n \sigma_c \quad (28)$$

Let $k_2^2 = \frac{uk}{A_s E_s}$

$$\frac{d^2 \sigma_{s1}}{dx^2} - k_2^2 \sigma_{s1} = -k_2^2 n \sigma_c \quad (29)$$

The homogeneous solution of Eq. (29) is:

$$\sigma_{s1H} = A \cosh k_2 x + B \sinh k_2 x \quad (30)$$

because of σ_c is also a function of (x), thus the particular solution is taken as the following:

$$\sigma_{s1 \rho} = C \sinh k_1 x + D \cosh k_1 x + E \quad (31)$$

Substitute $\sigma_{s1 \rho}$ & its 2nd derivative into eq. (29) to find the constants C, D, & E.

$$(\sigma_{s1 \rho})'' = k_1^2 C \sinh k_1 x + k_1^2 D \cosh k_1 x \quad (32)$$

substitute Eqs. (31 and 32) into Eq. (29);

$$k_1^2 C \sinh k_1 x + k_1^2 D \cosh k_1 x - k_2^2 C \sinh k_1 x - k_2^2 D \cosh k_1 x - k_2^2 E = -k_2^2 n \left[\left(\sigma f_u - \frac{\sigma_s \rho}{1+2n\rho} \right) \frac{\cosh k_1 x}{\cosh \frac{k_1 L}{2}} + \frac{\sigma_{s1 \rho}}{1+2n\rho} \right]$$

$$(k_1^2 - k_2^2) C \sinh k_1 x + (k_1^2 - k_2^2) D \cosh k_1 x - k_2^2 E =$$

$$-k_2^2 n \left[\left(\sigma f_u - \frac{\sigma_s \rho}{1+2n\rho} \right) \frac{\cosh k_1 x}{\cosh \frac{k_1 L}{2}} + \frac{\sigma_{s1 \rho}}{1+2n\rho} \right]$$

C=0;

$$(k_1^2 - k_2^2) D = -k_2^2 n \left(\sigma f_u - \frac{\sigma_s \rho}{1+2n\rho} \right) \frac{1}{\cosh \frac{k_1 L}{2}}$$

$$k_1^2 - k_2^2 = \frac{uk}{E_s A_s} (1 + 2n\rho) - \frac{uk}{E_s A_s} = \frac{uk}{E_s A_s} 2n\rho = k_2^2 2n\rho$$

$$D = \frac{-k_2^2 n \left(\sigma f_u - \frac{\sigma_s \rho}{1+2n\rho} \right)}{k_2^2 (2n\rho) \cosh \frac{k_1 L}{2}} = \frac{-(\sigma f_u - \frac{\sigma_s \rho}{1+2n\rho})}{2\rho \cosh \frac{k_1 L}{2}}$$

$$-k_2^2 E = -k_2^2 n \left(\frac{\sigma_s \rho}{1+2n\rho} \right)$$

$$E = \frac{\sigma_s \rho n}{1+2n\rho}$$

finally:

$$\sigma_{s1} = A \cosh k_2 x + B \sinh k_2 x + \left[\frac{-(\sigma f_u - \frac{\sigma_s \rho}{1+2n\rho})}{2\rho \cosh \frac{k_1 L}{2}} \right] \cosh k_1 x + \left[\frac{\sigma_s \rho n}{1+2n\rho} \right]$$

or

$$\sigma_{s1} = A \cosh k_2 x + B \sinh k_2 x - \frac{(\sigma f_u - \frac{\sigma_s \rho}{1+2n\rho})}{2\rho \cosh \frac{k_1 L}{2}} \cosh k_1 x + \frac{\sigma_s \rho n}{1+2n\rho} \quad (33)$$

for concrete without steel fiber; $\sigma f_u=0$;

$$\sigma_{s1} = A \cosh k_2 x + B \sinh k_2 x + \frac{\sigma_s \rho}{2(1+2n\rho)} \frac{\cosh k_1 x}{\cosh \frac{k_1 L}{2}} + \frac{\sigma_s \rho n}{1+2n\rho} \quad (34)$$

Applying B.C.:

$$\text{@ } x = \frac{L}{2}; \sigma_{s1} = 0$$

$$\text{and } x = -\frac{L}{2}; \sigma_{s1} = \sigma_s$$

$$A \cosh \frac{k_2 L}{2} + B \sinh \frac{k_2 L}{2} - \frac{(\sigma f_u - \frac{\sigma_s \rho}{1+2n\rho})}{2\rho \cosh \frac{k_1 L}{2}} \cosh \frac{k_1 L}{2} + \frac{\sigma_s \rho n}{1+2n\rho} = 0 \quad (35)$$

$$A \cosh \frac{k_2 L}{2} + B \sinh \frac{k_2 L}{2} - \frac{(\sigma f_u - \frac{\sigma_s \rho}{1+2n\rho})}{2\rho \cosh \frac{k_1 L}{2}} \cosh \frac{k_1 L}{2} + \frac{\sigma_s \rho n}{1+2n\rho} = 0 \quad (36)$$

adding the above two equations:

$$2A \cosh \frac{k_2 L}{2} - \frac{2(\sigma f_u - \frac{\sigma_s \rho}{1+2n\rho})}{2\rho} + \frac{2\sigma_s \rho n}{1+2n\rho} = \sigma_s$$

$$2A \cosh \frac{k_2 L}{2} - \frac{\sigma f_u}{\rho} + \frac{\sigma_s}{1+2n\rho} + \frac{2\sigma_s \rho n}{1+2n\rho} = \sigma_s$$

$$2A \cosh \frac{k_2 L}{2} - \frac{\sigma f_u}{\rho} + \frac{\sigma_s}{1+2n\rho} (1 + 2n\rho) = \sigma_s$$

$$A = \frac{\sigma f_u}{2\rho \cosh \frac{k_2 L}{2}} \quad (37)$$

for $\sigma f_u=0$; A=0

substitute in Eq. (35);

$$\frac{\sigma f_u}{2\rho \cosh \frac{k_2 L}{2}} \cosh \frac{k_2 L}{2} + B \sinh \frac{k_2 L}{2} - \frac{\sigma f_u}{2\rho} + \frac{\sigma_s}{2(1+2n\rho)} + \frac{\sigma_s \rho n}{1+2n\rho} = 0$$

$$\frac{\sigma f_u}{2\rho} + B \sinh \frac{k_2 L}{2} - \frac{\sigma f_u}{2\rho} + \frac{\sigma_s}{2(1+2n\rho)} (1 + 2n\rho) = 0$$

$$B = \frac{-\sigma_s}{2 \sinh \frac{k_2 L}{2}} \quad (38)$$

Finally:

$$\sigma_{s1} = \frac{\sigma f_u}{2\rho \cosh \frac{k_2 L}{2}} \cosh k_2 x - \frac{\sigma_s}{2 \sinh \frac{k_2 L}{2}} \sinh k_2 x - \frac{(\sigma f_u - \frac{\sigma_s \rho}{1+2n\rho})}{2\rho \cosh \frac{k_1 L}{2}} \cosh k_1 x + \frac{\sigma_s \rho n}{1+2n\rho}$$

or

$$\sigma_{s1} = \frac{\sigma f_u \cosh k_2 x}{2\rho \cosh \frac{k_2 L}{2}} - \frac{\sigma_s \sinh k_2 x}{2 \sinh \frac{k_2 L}{2}} - \left(\sigma f_u - \frac{\sigma_s \rho}{1+2n\rho} \right) \frac{\cosh k_1 x}{2\rho \cosh \frac{k_1 L}{2}} + \frac{\sigma_s \rho n}{1+2n\rho} \quad (39)$$

Check:

$$\text{@ } x = \frac{L}{2}; \sigma_{s1} = \frac{\sigma f_u}{2\rho} - \frac{\sigma_s}{2} - \frac{\sigma f_u}{2\rho} + \frac{\sigma_s}{2(1+2n\rho)} + \frac{\sigma_s \rho n}{1+2n\rho} \quad \text{@}$$

$$\sigma_{s1} = \frac{\sigma f_u}{2\rho} - \frac{\sigma_s}{2} - \frac{\sigma f_u}{2\rho} - \frac{\sigma_s}{2} = 0$$

$$\text{@ } x = -\frac{L}{2}; \sigma_{s1} = \frac{\sigma f_u}{2\rho} + \frac{\sigma_s}{2} - \frac{\sigma f_u}{2\rho} + \frac{\sigma_s}{2} = \sigma_s$$

By the same way. The derivation of Eq. (2) is combined with Eq. (11) to get;

$$\frac{d^2\sigma_{s2}}{dx^2} - k_2^2 \sigma_{s2} = -k_2^2 n \sigma_c \tag{40}$$

By the same previous procedures, the general solution is:

$$\sigma_{s2} = A \cosh k_2 x + B \sinh k_2 x + \frac{(\sigma f_u - \frac{\sigma_s \rho}{1+2n\rho})}{2\rho \cosh \frac{k_1 L}{2}} \cosh k_1 x + \frac{\sigma_s \rho n}{1+2n\rho} \tag{41}$$

The B.C. are:

$$@x = \frac{L}{2}; \sigma_{s2} = \sigma_s$$

$$@x = -\frac{L}{2}; \sigma_{s2} = 0$$

$$A \cosh \frac{k_2 L}{2} + B \sinh \frac{k_2 L}{2} - \frac{(\sigma f_u - \frac{\sigma_s \rho}{1+2n\rho})}{2\rho \cosh \frac{k_1 L}{2}} \cosh k_1 x + \frac{\sigma_s \rho n}{1+2n\rho} = \sigma_s \tag{42}$$

$$A \cosh \frac{k_2 L}{2} - B \sinh \frac{k_2 L}{2} - \frac{(\sigma f_u - \frac{\sigma_s \rho}{1+2n\rho})}{2\rho \cosh \frac{k_1 L}{2}} \cosh k_1 x + \frac{\sigma_s \rho n}{1+2n\rho} = 0 \tag{43}$$

adding the above two equations:

$$2A \cosh \frac{k_2 L}{2} - \frac{2\sigma f_u}{2\rho} + 2 \frac{\sigma_s \rho}{2\rho(1+2n\rho)} + \frac{2\sigma_s \rho n}{1+2n\rho} = \sigma_s$$

$$A \cosh \frac{k_2 L}{2} - \frac{\sigma f_u}{\rho} + \frac{\sigma_s}{(1+2n\rho)} (1+2n\rho) = \sigma_s$$

$$A = \frac{\sigma f_u}{2\rho \cosh \frac{k_2 L}{2}} \tag{44}$$

for $\sigma f_u = 0$; $A = 0$

sub. in Eq. (42);

$$\frac{\sigma f_u}{2\rho \cosh \frac{k_2 L}{2}} \cosh \frac{k_2 L}{2} - B \sinh \frac{k_2 L}{2} - \frac{\sigma f_u}{2\rho} + \frac{\sigma_s}{2(1+2n\rho)} + \frac{\sigma_s \rho n}{1+2n\rho} = 0$$

$$\frac{\sigma f_u}{2\rho} - B \sinh \frac{k_2 L}{2} - \frac{\sigma f_u}{2\rho} + \frac{\sigma_s (1+2n\rho)}{2(1+2n\rho)} = 0$$

$$B = \frac{\sigma_s}{2 \sinh \frac{k_2 L}{2}} \tag{45}$$

Finally:

$$\sigma_{s2} = \frac{\sigma f_u \cosh k_2 x}{2\rho \cosh \frac{k_2 L}{2}} + \frac{\sigma_s \sinh k_2 x}{2 \sinh \frac{k_2 L}{2}} - \left(\sigma f_u - \frac{\sigma_s \rho}{1+2n\rho}\right) \frac{\cosh k_1 x}{2\rho \cosh \frac{k_1 L}{2}} + \frac{\sigma_s \rho n}{1+2n\rho} \tag{46}$$

Check:

$$@x = \frac{L}{2}; \sigma_{s2} = \frac{\sigma f_u}{2\rho} + \frac{\sigma_s}{2} - \frac{\sigma f_u}{2\rho} + \left(\frac{\sigma_s}{2(1+2n\rho)}\right) + \frac{\sigma_s \rho n}{1+2n\rho}$$

$\sigma_{s2} = \sigma_s$

$$@x = -\frac{L}{2}; \sigma_{s2} = \frac{\sigma f_u}{2\rho} - \frac{\sigma_s}{2} - \frac{\sigma f_u}{2\rho} + \frac{\sigma_s}{2} = 0$$

The bond stresses (τ_1 & τ_2) at $x = \frac{L}{2}$ & $x = -\frac{L}{2}$ are determined from Eqs. (2 & 3):

$$\tau_1 = \frac{A_s}{u} \frac{d\sigma_{s1}}{dx} \tag{47}$$

$$\tau_2 = \frac{A_s}{u} \frac{d\sigma_{s2}}{dx} \tag{48}$$

from Eq. (39);

$$\frac{d\sigma_{s1}}{dx} = \left[\frac{\sigma f_u}{2\rho} k_2 \frac{\sinh k_2 x}{\cosh \frac{k_2 L}{2}} - \frac{\sigma_s k_2}{2} \frac{\cosh k_2 x}{\sinh \frac{k_2 L}{2}} - \left(\sigma f_u - \frac{\sigma_s \rho}{1+2n\rho}\right) k_1 \frac{\sinh k_1 x}{2\rho \cosh \frac{k_1 L}{2}} \right] \tag{49}$$

$$\tau_1 = \frac{A_s}{u} \left[\frac{\sigma f_u}{2\rho} k_2 \frac{\sinh k_2 x}{\cosh \frac{k_2 L}{2}} - \frac{\sigma_s k_2}{2} \frac{\cosh k_2 x}{\sinh \frac{k_2 L}{2}} - \left(\sigma f_u - \frac{\sigma_s \rho}{1+2n\rho}\right) k_1 \frac{\sinh k_1 x}{2\rho \cosh \frac{k_1 L}{2}} \right]$$

from Eq. (46);

$$\tau_2 = \frac{A_s}{u} \left[\frac{\sigma f_u}{2\rho} k_2 \frac{\sinh k_2 x}{\cosh \frac{k_2 L}{2}} + \frac{\sigma_s k_2}{2} \frac{\cosh k_2 x}{\sinh \frac{k_2 L}{2}} - \left(\sigma f_u - \frac{\sigma_s \rho}{1+2n\rho}\right) k_1 \frac{\sinh k_1 x}{2\rho \cosh \frac{k_1 L}{2}} \right] \tag{50}$$

For the special case:

when $\rho = \infty$; at $x = \pm \frac{L}{2}$; concrete cracks and $A_c = 0$, then $\rho = \infty$

$$\frac{\sigma_s \rho}{1+2n\rho} = \frac{\sigma_s}{1+2n} = \frac{\sigma_s}{2n}$$

from Eq. (24);

$$\sigma_c = \left(\sigma f_u - \frac{\sigma_s}{2n}\right) \frac{\cosh k_1 x}{\cosh \frac{k_1 L}{2}} + \frac{\sigma_s}{2n} \tag{51}$$

$$@x = \pm \frac{L}{2}; \sigma_c = \left(\sigma f_u - \frac{\sigma_s}{2n}\right) + \frac{\sigma_s}{2n} = \sigma f_u$$

$$@x = 0; \sigma_c = \left(\sigma f_u - \frac{\sigma_s}{2n}\right) \frac{1}{\cosh \frac{k_1 L}{2}} + \frac{\sigma_s}{2n}$$

$$\sigma_c = \frac{\sigma f_u}{\cosh \frac{k_1 L}{2}} + \frac{\sigma_s}{2n} \left(1 - \frac{1}{\cosh \frac{k_1 L}{2}}\right)$$

for concrete without fiber, $\sigma f_u = 0$;

$$@x = \frac{L}{2}; \sigma_c = 0$$

$$@x = -\frac{L}{2}; \sigma_c = \frac{\sigma_s}{2n} \left(1 - \frac{1}{\cosh \frac{k_1 L}{2}}\right)$$

from Eq. (39);

$$\sigma_{s1} = \frac{\sigma f_u \cosh k_2 x}{2\rho \cosh \frac{k_2 L}{2}} - \frac{\sigma_s \sinh k_2 x}{2 \sinh \frac{k_2 L}{2}} - \left(\sigma f_u - \frac{\sigma_s}{2n}\right) \frac{\cosh k_1 x}{2\rho \cosh \frac{k_1 L}{2}} + \frac{\sigma_s n}{2n}$$

$$\sigma_{s1} = \frac{-\sigma_s \sinh k_2 x}{2 \sinh \frac{k_2 L}{2}} + \frac{\sigma_s}{2} \tag{52}$$

$$@x = \frac{L}{2}; \sigma_{s1} = 0$$

$$@x = -\frac{L}{2}; \sigma_{s1} = \frac{\sigma_s}{2} + \frac{\sigma_s}{2} = \sigma_s$$

$$@x = 0; \sigma_{s1} = \frac{\sigma_s}{2}$$

and from Eq. (49);

$$\tau_1 = \frac{A_s}{u} \left[\frac{-\sigma_s k_2 \cosh k_2 x}{2 \sinh \frac{k_2 L}{2}} \right] \tag{53}$$

$$\sigma_{s2} = \frac{\sigma f_u \cosh k_2 x}{2\rho \cosh \frac{k_2 L}{2}} + \frac{\sigma_s \sinh k_2 x}{2 \sinh \frac{k_2 L}{2}} - \left(\sigma f_u - \frac{\sigma_s}{2n}\right) \frac{\cosh k_1 x}{2\rho \cosh \frac{k_1 L}{2}} + \frac{\sigma_s n}{2n}$$

$$\sigma_{s2} = \frac{\sigma_s \sinh k_2 x}{2 \sinh \frac{k_2 L}{2}} + \frac{\sigma_s}{2} = \frac{\sigma_s}{2} \left[1 + \frac{\sinh k_2 x}{\sinh \frac{k_2 L}{2}}\right] \tag{54}$$

from Eq. (50);

$$\tau_2 = \frac{A_s}{u} \left[\frac{\sigma_s k_2 \cosh k_2 x}{2 \sinh \frac{k_2 L}{2}} \right] \tag{55}$$

@ $x = \frac{L}{2}$; $\sigma_{s2} = \sigma_s$

@ $x = -\frac{L}{2}$; $\sigma_{s2} = \frac{-\sigma_s}{2} + \frac{\sigma_s}{2} = 0$

@ $x = 0$; $\sigma_{s2} = \frac{\sigma_s}{2}$

@ $x = \mp \frac{L}{2}$; $\tau_1 = \frac{A_s}{u} \left(\frac{-\sigma_s k_2}{2} \right) \coth \frac{k_2 L}{2}$

$\tau_2 = \frac{A_s}{u} \left(\frac{\sigma_s k_2}{2} \right) \coth \frac{k_2 L}{2}$

@ $x = 0$; $\tau_1 = \frac{A_s}{u} \left(\frac{-\sigma_s k_2}{2} \right) \frac{1}{\sinh \frac{k_2 L}{2}}$

$\tau_2 = \frac{A_s}{u} \left(\frac{\sigma_s k_2}{2} \right) \frac{1}{\sinh \frac{k_2 L}{2}}$

3. RESULTS AND DISCUSSION

Effect of steel fiber content is considered on the bond stress between steel bars and surrounding fibrous concrete and concrete stress at the lap splice, taking into account the following variables:

- 1- Steel fiber content (Qf%).
- 2- Value of modulus of displacement k N/mm3.
- 3- Reinforcement index (ρ%).
- 4- Bar diameter (d_b) mm.
- 5- Steel bar yield strength (f_y) N/mm².
- 6- Compressive strength of concrete f_c' N/mm².

Excel data sheets are prepared to apply equations of concrete stress (σ_c), steel stress (σ_s), and bond stress (τ). The value of these stresses is determined along the bar splice length considering the variables mentioned above.

Table 1. Sample data sheet for calculating concrete stress (σ_c).

K(N/mm ³)=	50	100	150	50	100	150	50	100	150	50	100	150
L (mm) =	500	500	500	500	500	500	500	500	500	500	500	500
Fy(N/mm ²)=	420	420	420	420	420	420	420	420	420	420	420	420
Rho % =	1	1	1	1	1	1	1	1	1	1	1	1
Qf (fiber) %=	0	0	0	0.5	0.5	0.5	1	1	1	2	2	2
L/D Fiber =	100	100	100	100	100	100	100	100	100	100	100	100
df fiber =	1	1	1	1	1	1	1	1	1	1	1	1
fc'(N/mm ²)=	28	28	28	28	28	28	28	28	28	28	28	28
Es(N/mm ²)=	200000	200000	200000	200000	200000	200000	200000	200000	200000	200000	200000	200000
bar diameter=	10	10	10	10	10	10	10	10	10	10	10	10
F=	0	0	0	0.5	0.5	0.5	1	1	1	2	2	2
Sigma fu=	0	0	0	1.7015	1.7015	1.7015	3.403	3.403	3.403	6.806	6.806	6.806
u=	31.4159	31.4159	31.4159	31.4159	31.4159	31.4159	31.4159	31.4159	31.4159	31.4159	31.4159	31.4159
As=	78.53975	78.53975	78.53975	78.53975	78.53975	78.53975	78.53975	78.53975	78.53975	78.53975	78.53975	78.53975
Ec=	25034.099	25034.099	25034.099	25034.099	25034.099	25034.099	25034.1	25034.1	25034.099	25034.099	25034.1	25034.099
n=	7.9891032	7.9891032	7.9891032	7.9891032	7.9891032	7.9891032	7.989103	7.989103	7.9891032	7.9891032	7.989103	7.9891032
K2^2=	0.00010	0.00020	0.00030	0.00010	0.00020	0.00030	0.00010	0.00020	0.00030	0.00010	0.00020	0.00030
K1^2=	0.000116	0.000232	0.0003479	0.000116	0.000232	0.0003479	0.000116	0.000232	0.0003479	0.000116	0.000232	0.0003479
K1*L/2=	2.6923295	3.8075288	4.6632514	2.6923295	3.8075288	4.6632514	2.692329	3.807529	4.6632514	2.6923295	3.807529	4.6632514
K2*L/2=	2.5	3.5355339	4.330127	2.5	3.5355339	4.330127	2.5	3.535534	4.330127	2.5	3.535534	4.330127
Fy*Rho/(1+2nRho)=	3.62137	3.62137	3.62137	3.62137	3.62137	3.62137	3.62137	3.62137	3.62137	3.62137	3.62137	3.62137
Sfu - above =	-3.62137	-3.62137	-3.62137	-1.91987	-1.91987	-1.91987	-0.21837	-0.21837	-0.21837	-0.21837	3.18463	3.18463
K2=	0.01	0.0141421	0.0173205	0.01	0.0141421	0.0173205	0.01	0.014142	0.0173205	0.01	0.014142	0.0173205
K1=	0.0107693	0.0152301	0.018653	0.0107693	0.0152301	0.018653	0.010769	0.01523	0.018653	0.0107693	0.01523	0.018653
Cosh(K1L/2)=	7.4168779	22.530603	52.994771	7.4168779	22.530603	52.994771	7.416878	22.5306	52.994771	7.4168779	22.5306	52.994771
Cosh(K2L/2)=	6.1322895	17.171237	37.98355	6.1322895	17.171237	37.98355	6.132289	17.17124	37.98355	6.1322895	17.17124	37.98355
-	-	-	-	-	-	-	-	-	-	-	-	-
X	Sc(Concrete)	Sc(Concrete)	Sc(Concrete)	Sc(Concrete)	Sc(Concrete)	Sc(Concrete)	Sc(Concrete)	Sc(Concrete)	Sc(Concrete)	Sc(Concrete)	Sc(Concrete)	Sc(Concrete)
-250	0	0	0	1.7015	1.7015	1.7015	3.403	3.403	3.403	6.806	6.806	6.806
-200	1.4891048	1.9273371	2.1956344	2.4909492	2.7232781	2.865516	3.492794	3.519219	3.5353976	5.4964824	5.111101	4.8751608
-150	2.3448858	2.823921	3.0585701	2.9446417	3.1986023	3.3230015	3.544398	3.573284	3.587433	4.7439093	4.322646	4.1162959
-100	2.8215263	3.2352882	3.3954314	3.1973327	3.4166887	3.5015886	3.573139	3.598089	3.6077458	4.3247519	3.96089	3.8200602
-50	3.0605979	3.4117395	3.5210979	3.3240766	3.5102344	3.5682107	3.587555	3.608729	3.6153236	4.1145126	3.805719	3.7095492
0	3.1331093	3.4606389	3.5530355	3.3625185	3.5361584	3.5851425	3.591928	3.611678	3.6172494	4.0507461	3.762717	3.6814633
50	3.0605979	3.4117395	3.5210979	3.3240766	3.5102344	3.5682107	3.587555	3.608729	3.6153236	4.1145126	3.805719	3.7095492
100	2.8215263	3.2352882	3.3954314	3.1973327	3.4166887	3.5015886	3.573139	3.598089	3.6077458	4.3247519	3.96089	3.8200602
150	2.3448858	2.823921	3.0585701	2.9446417	3.1986023	3.3230015	3.544398	3.573284	3.587433	4.7439093	4.322646	4.1162959
200	1.4891048	1.9273371	2.1956344	2.4909492	2.7232781	2.865516	3.492794	3.519219	3.5353976	5.4964824	5.111101	4.8751608
250	0	0	0	1.7015	1.7015	1.7015	3.403	3.403	3.403	6.806	6.806	6.806

bar diameter=	10	10	10	10	10	10	10	10	10	10	10	10
F=	0	0	0	0.5	0.5	0.5	1	1	1	2	2	2
Sigma fu=	0	0	0	1.7015	1.7015	1.7015	3.403	3.403	3.403	6.806	6.806	6.806
u=	31.4159	31.4159	31.4159	31.4159	31.4159	31.4159	31.4159	31.4159	31.4159	31.4159	31.4159	31.4159
As=	78.53975	78.53975	78.53975	78.53975	78.53975	78.53975	78.53975	78.53975	78.53975	78.53975	78.53975	78.53975
Ec=	25034.099	25034.099	25034.099	25034.099	25034.099	25034.099	25034.1	25034.1	25034.099	25034.099	25034.1	25034.099
n=	7.9891032	7.9891032	7.9891032	7.9891032	7.9891032	7.9891032	7.989103	7.989103	7.9891032	7.9891032	7.989103	7.9891032
K2^2=	0.00010	0.00020	0.00030	0.00010	0.00020	0.00030	0.00010	0.00020	0.00030	0.00010	0.00020	0.00030
K1^2=	0.000116	0.000232	0.0003479	0.000116	0.000232	0.0003479	0.000116	0.000232	0.0003479	0.000116	0.000232	0.0003479
K1*L/2=	2.6923295	3.8075288	4.6632514	2.6923295	3.8075288	4.6632514	2.692329	3.807529	4.6632514	2.6923295	3.807529	4.6632514
K2*L/2=	2.5	3.5355339	4.330127	2.5	3.5355339	4.330127	2.5	3.535534	4.330127	2.5	3.535534	4.330127
Fy*Rho/(1+2nRho)=	3.62137	3.62137	3.62137	3.62137	3.62137	3.62137	3.62137	3.62137	3.62137	3.62137	3.62137	3.62137
Sfu - above =	-3.62137	-3.62137	-3.62137	-1.91987	-1.91987	-1.91987	-0.21837	-0.21837	-0.21837	3.18463	3.18463	3.18463
K2=	0.01	0.0141421	0.0173205	0.01	0.0141421	0.0173205	0.01	0.014142	0.0173205	0.01	0.014142	0.0173205
K1=	0.0107693	0.0152301	0.018653	0.0107693	0.0152301	0.018653	0.010769	0.01523	0.018653	0.0107693	0.01523	0.018653
Cosh(K1L/2)=	7.4168779	22.530603	52.994771	7.4168779	22.530603	52.994771	7.416878	22.5306	52.994771	7.4168779	22.5306	52.994771
Cosh(K2L/2)=	6.1322895	17.171237	37.98355	6.1322895	17.171237	37.98355	6.132289	17.17124	37.98355	6.1322895	17.17124	37.98355
Sinh(K1L/2)=	7.3491549	22.5084	52.985336	7.3491549	22.5084	52.985336	7.349155	22.5084	52.985336	7.3491549	22.5084	52.985336
Sinh(K2L/2)=	6.0502045	17.142093	37.970384	6.0502045	17.142093	37.970384	6.050204	17.14209	37.970384	6.0502045	17.14209	37.970384
-	-	-	-	-	-	-	-	-	-	-	-	-
-	-	-	-	-	-	-	-	-	-	-	-	-
-	-	-	-	-	-	-	-	-	-	-	-	-
X	σ_1 (Steel)	σ_1 (Steel)	σ_1 (Steel)	σ_1 (Steel)	σ_1 (Steel)	σ_1 (Steel)	σ_1 (Steel)	σ_1 (Steel)	σ_1 (Steel)	σ_1 (Steel)	σ_1 (Steel)	σ_1 (Steel)
-250	420	420	420	420	420	420	420	420	420	420	420	420
-200	261.43153	216.90355	188.47724	263.53332	219.16514	190.79626	265.6351	221.4267	193.11528	269.8387	225.9499	197.75332
-150	166.66209	119.16761	94.025607	169.30994	121.3961	95.936336	171.9578	123.6246	97.847064	177.25351	128.0816	101.66852
-100	109.71441	71.941216	55.369382	112.33169	73.663016	56.58955	114.949	75.38482	57.809717	120.18352	78.82842	60.250053
-50	75.0571	48.815601	39.356332	77.527042	50.136469	40.13422	79.99698	51.45734	40.912109	84.93687	54.09907	42.467885
0	53.344534	36.968057	32.348223	55.747359	38.146588	32.982661	58.15018	39.32512	33.617099	62.955835	41.68218	34.885976
50	38.883111	30.010446	28.533878	41.353054	31.331314	29.311766	43.823	32.65218	30.089654	48.762882	35.29392	31.64543
100	28.132954	24.529967	25.087475	30.750232	26.251767	26.307643	33.36751	27.97357	27.527811	38.602065	31.41717	29.968146
150	18.849334	18.440293	20.117388	21.49719	20.66879	22.028117	24.14505	22.89729	23.938846	29.440758	27.35428	27.760303
200	9.6579908	10.36274	11.959318	11.759785	12.62433	14.278338	13.86158	14.88592	16.597359	18.065167	19.4091	21.235401
250	-2.84E-14	-2.842E-14	0	0	0	0	0	0	0	5.684E-14	0	0

Tables (1-3) show samples of calculations. 45 datasheets are prepared for each (σ_c, σ_s & τ) to cover the effect of all variables.

Figs. (6 and 7) show the variation of concrete stress (σ_c) along the length of the bar splice ($-\frac{L}{2}$ to $\frac{L}{2}$) for concrete without and with steel fiber ($Q_f=1\%$). The maximum stress is obtained at center $x=0$ and minimum at ($x = \pm \frac{L}{2}$).

Figs. (8 and 9) show the variation of bond stress (τ_1) between the steel bar and surrounding concrete for concrete without steel fiber and with steel fiber content ($Q_f=1\%$). The maximum value is obtained at ($x = \pm \frac{L}{2}$), and minimum value at ($x = \frac{L}{2}$).

Figs. (10 and 11) show the variation of steel stress (σ_s) in the splice bar for both plain ($Q_f=0$) and fibrous concrete ($Q_f=1\%$). The maximum value is ($\sigma_s=f_y$) at ($x = -\frac{L}{2}$) and minimum value is ($\sigma_s=0$) at ($x = \frac{L}{2}$).

The value of τ_2 is the same as (τ_1) but in opposite sides, i.e., at ($\tau_2=\tau_1$). Also ($\sigma_s=f_y$) at ($x=\frac{L}{2}$) and equal to zero at ($x = -\frac{L}{2}$).

Figs. (12-15) show the effect of fiber content on the maximum concrete stress (σ_{cmax}) for steel bar content ($\rho=1,5,10\%$ and ∞). The value of (σ_{cmax}) increased linearly with the increase of (ρ), the slope of the lines decreased with the increase in the value of displacement modulus from (k) to $(100 \frac{N}{mm^2})$, the effect is negligible at ($k=150 N/mm^2$), the same behavior is noticed for ($\rho=5\&10\%$), but when ($\rho = \infty$), the effect of steel fiber content (Q_f) and steel bar reinforcement index ($\rho\%$) are neglected, and concrete stress becomes constant.

Fig. (16) shows the relation between reinforcement ratio (ρ) and maximum concrete stress (σ_{cmax}), for steel fiber content ($Q_f=0\%$), the concrete stress increased nonlinearly (parabolic) with increasing of ($\rho\%$). Also, increasing value of (k) has a small effect on (σ_{cmax}). The same behavior is obtained for other steel fiber content, as shown in Figs. (18-19).

Figs. (20-23) show that the bar diameter has a negligible effect on maximum concrete stress for all steel fiber content (Q_f) and steel reinforcement content (ρ).

Fig. (24) shows that the maximum concrete stress (σ_{cmax}) increased linearly with (F_y); this effect is increased when the

value of (ρ) is increased. The same behavior is noticed in fibrous concrete, as shown in Figs. (25-27) .

Figs. (28-31) show that the maximum concrete stress (σ_{max}) increased linearly with concrete compressive strength (f_c'); the effect is reduced when (ρ) increased from (1& to 5 & 10%) and became negligible at ($\rho=\infty$).

Fig. (32) shows the relation of maximum bond stress (τ_{max}) and steel fiber content (Qf) for ($\rho=1\%$); value of (τ_{max}) decreased linearly with increasing of (Qf) for all values of (k) and (ρ), as shown in Figs. (33-35).

Figs. (36-39) show that bond stress (τ_{max}) decreased with increasing of ($\rho\%$) for all values of (Qf & k). Also, using of larger bar diameter (d_b) causes a linear increase in bond stress (τ_{max}) as shown in Figs. (40-43).

Figs. (44-47) show that value of (τ_{max}) increased with increasing of (f_y) for ($\rho=1,5,10\%$ and ∞) for plain concrete (Qf=0) and fibrous concrete (Qf=0.5,1&2%).

Figs. (48-51) show the effect of concrete compressive strength (f_{c1}) on the maximum bond stress (τ_{max}) for steel reinforcement content ($\rho=1,5,10\%$ and ∞). The effect is negligible at ($\rho=\infty$).

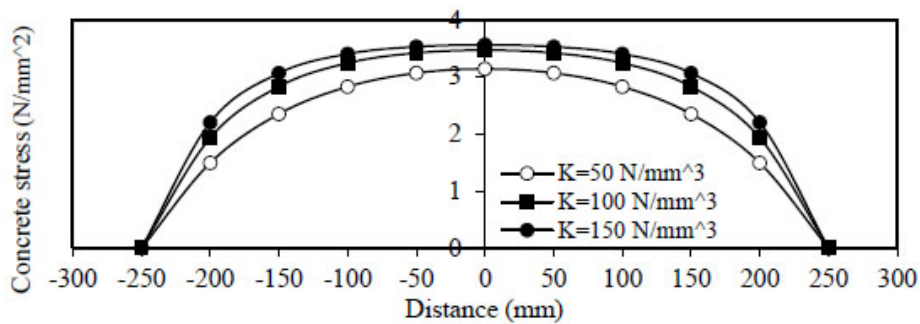


Fig. (6). Distribution of concrete stress, Rho=1%, Qf=0%.

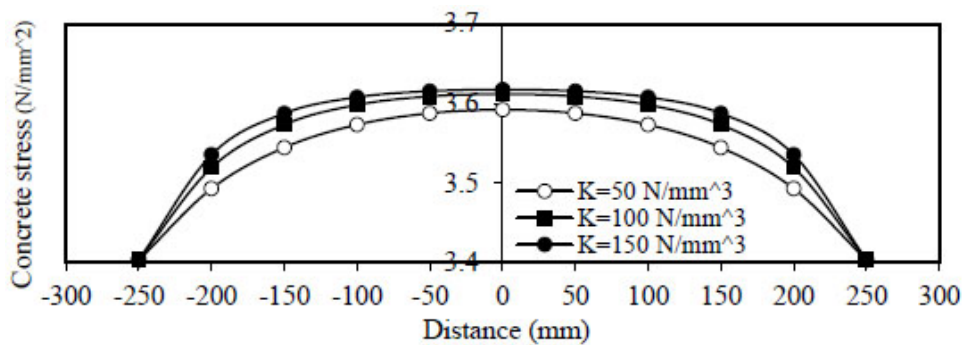


Fig. (7). Distribution of concrete stress, Rho=1%, Qf=1%.

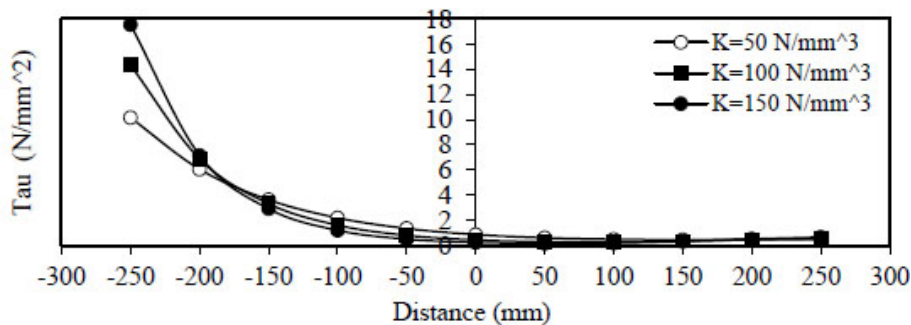


Fig. (8). Distribution of bond stress, Rho=1%, Qf=0%.

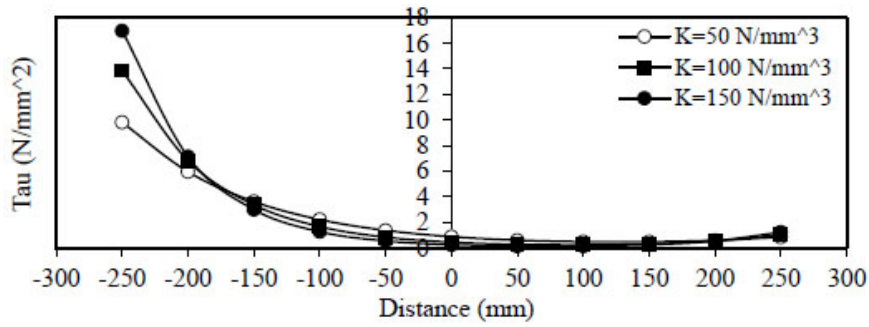


Fig. (9). Distribution of bond stress, Rho=1%, Qf=1%.

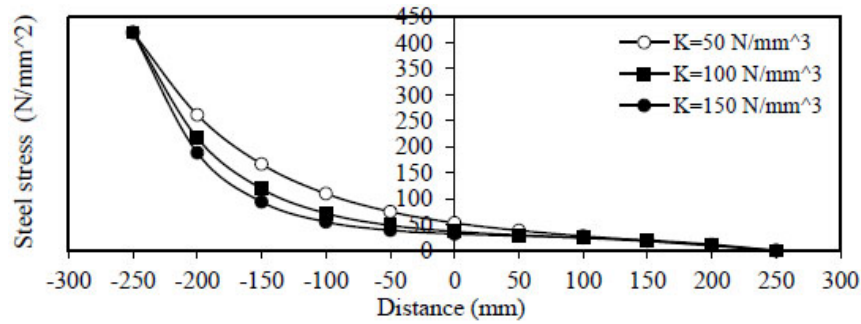


Fig. (10). Distribution of steel stress, Rho=1%, Qf=0%.

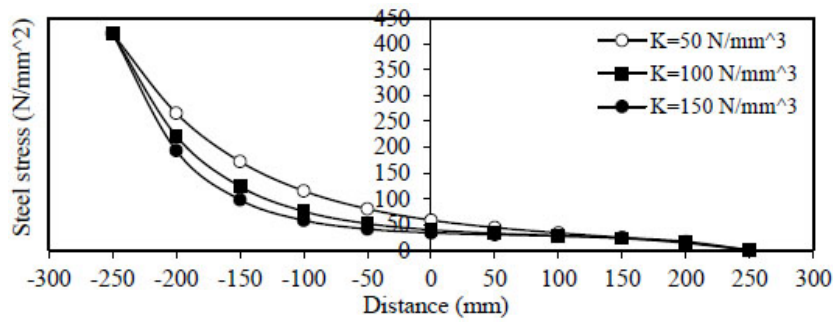


Fig. (11). Distribution of steel stress, Rho=1%, Qf=1%.

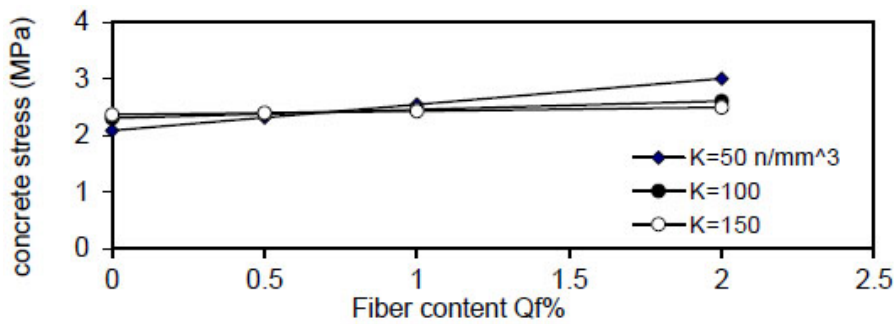


Fig. (12). Relation of Qf versus concrete stress (Rho=1%).

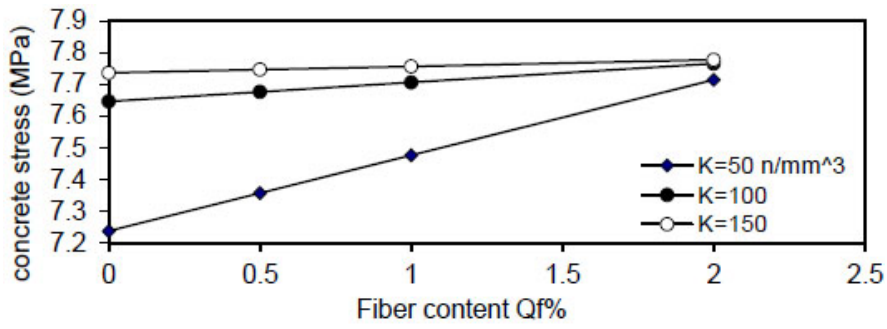


Fig. (13). Relation of Qf versus concrete stress (Rho=5%).

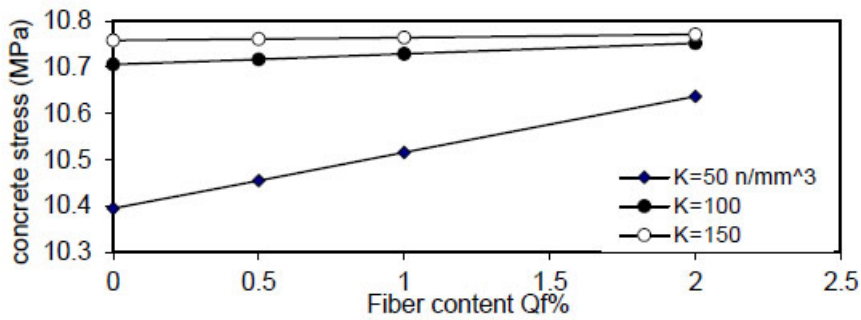


Fig. (14). Relation of Qf versus concrete stress (Rho=10%).

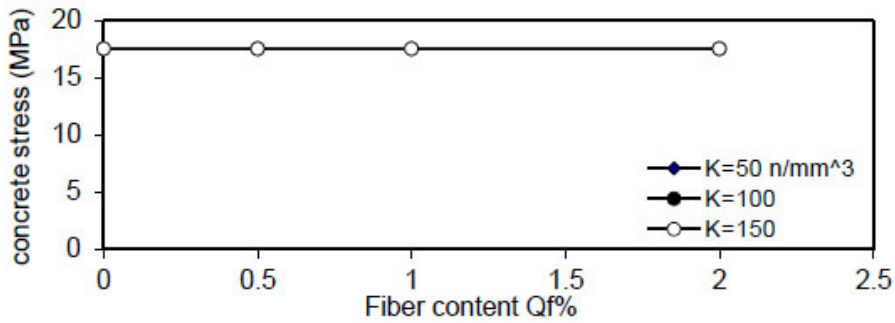


Fig. (15). Relation of Qf versus concrete stress (Rho=Infinity).

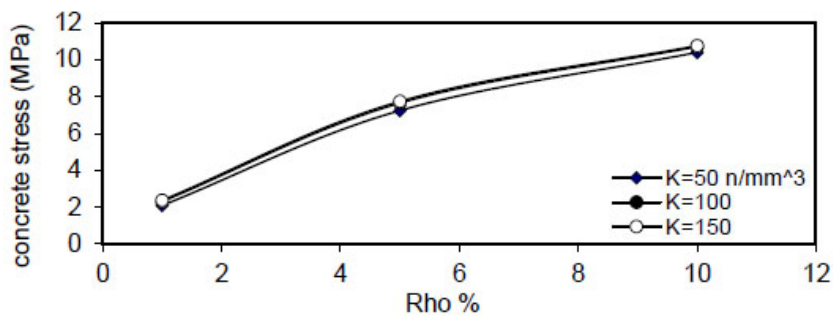


Fig. (16). Relation of (Rho %) versus concrete stress (Qf=0%).

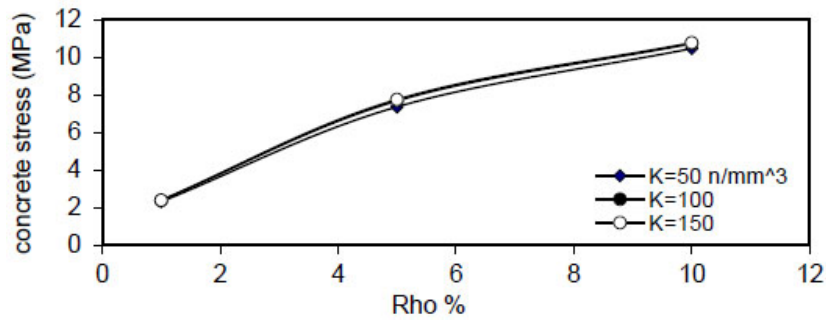


Fig. (17). Relation of (Rho %) versus concrete stress (Qf=0.5%).

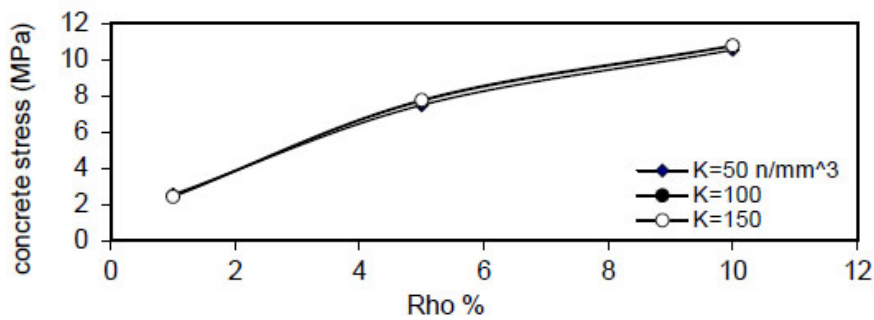


Fig. (18). Relation of (Rho %) versus concrete stress (Qf=1%).

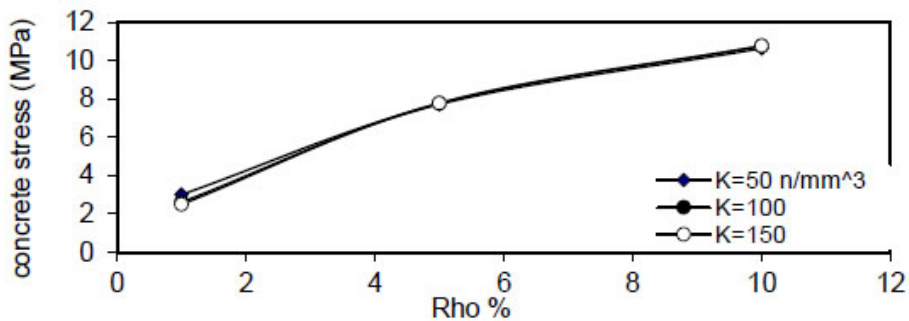


Fig. (19). Relation of (Rho %) versus concrete stress (Qf=2%).

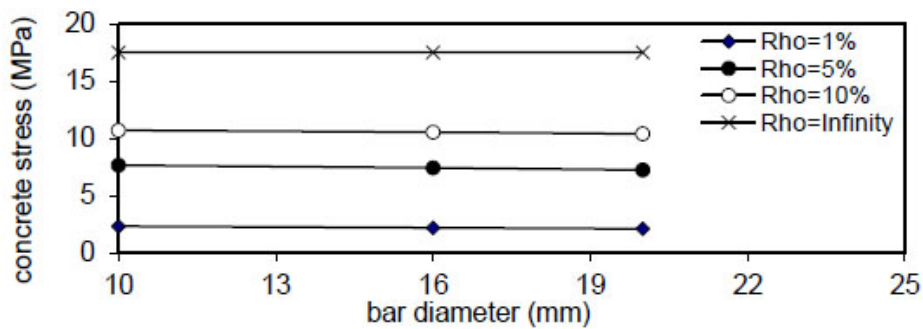


Fig. (20). Relation of bar diameter versus concrete stress (Qf=0%).

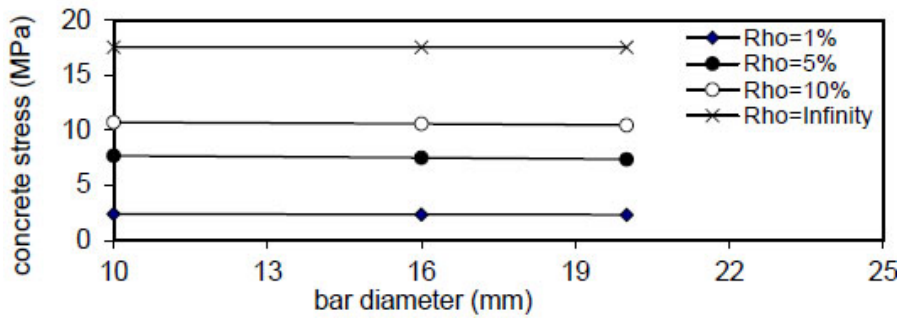


Fig. (21). Relation of bar diameter versus concrete stress (Qf=0.5%).

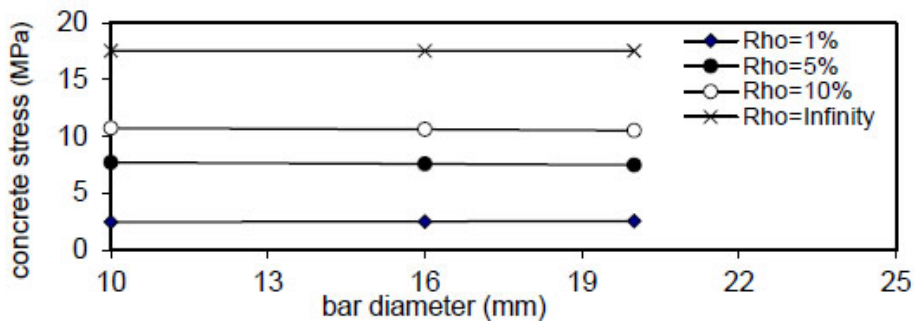


Fig. (22). Relation of bar diameter versus concrete stress (Qf=1%).

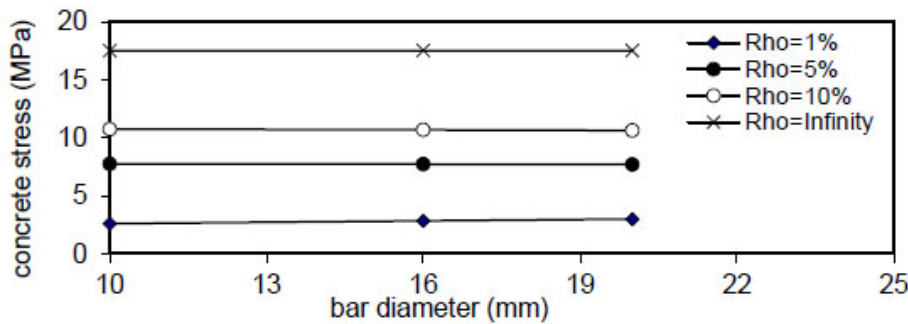


Fig. (23). Relation of bar diameter versus concrete stress (Qf=2%).

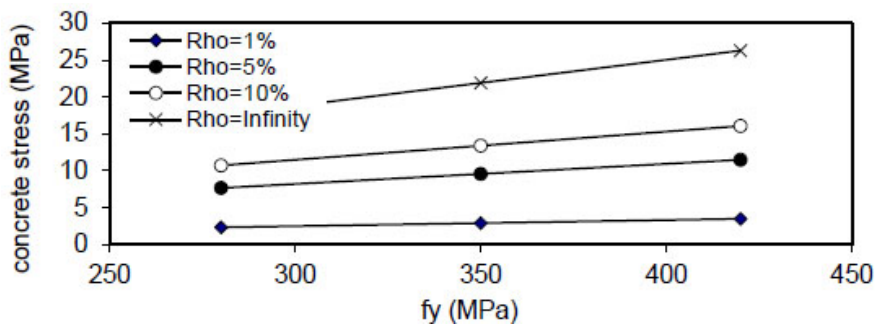


Fig. (24). Relation of fy versus concrete stress (Qf=0%).

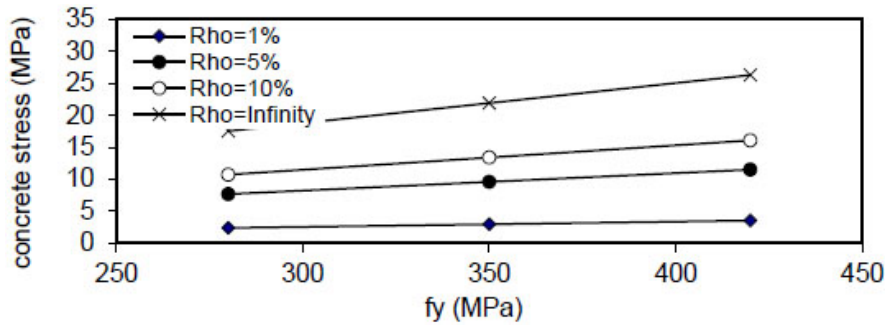


Fig. (25). Relation of f_y versus concrete stress ($Q_f=0.5\%$).

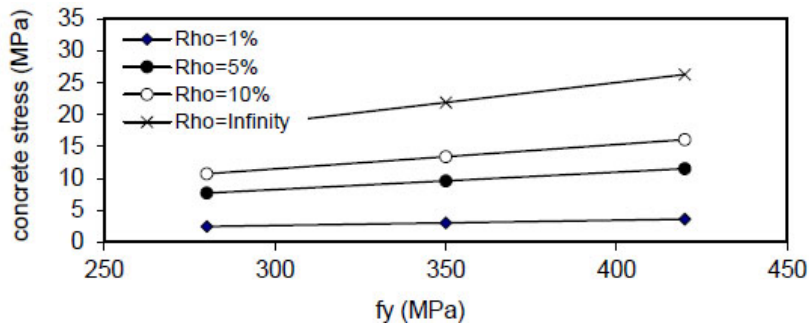


Fig. (26). Relation of f_y versus concrete stress ($Q_f=1\%$).

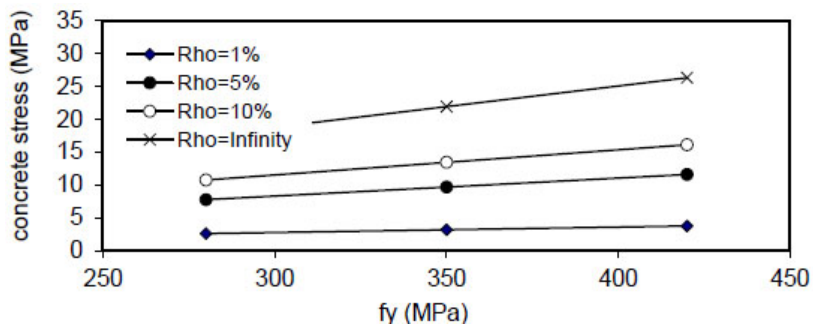


Fig. (27). Relation of f_y versus concrete stress ($Q_f=2\%$).

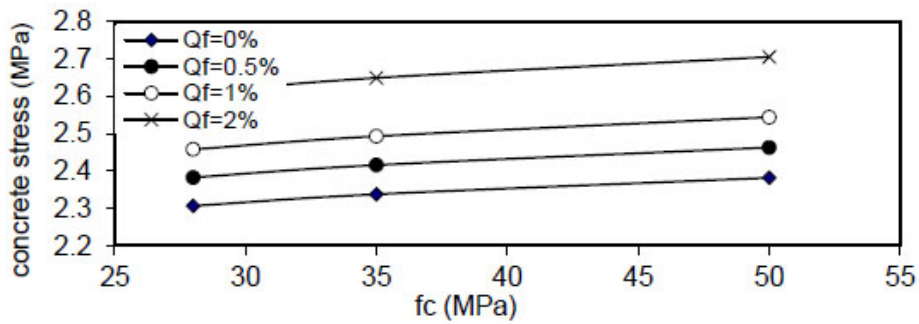


Fig. (28). Relation of f_c versus concrete stress ($\rho=1\%$).

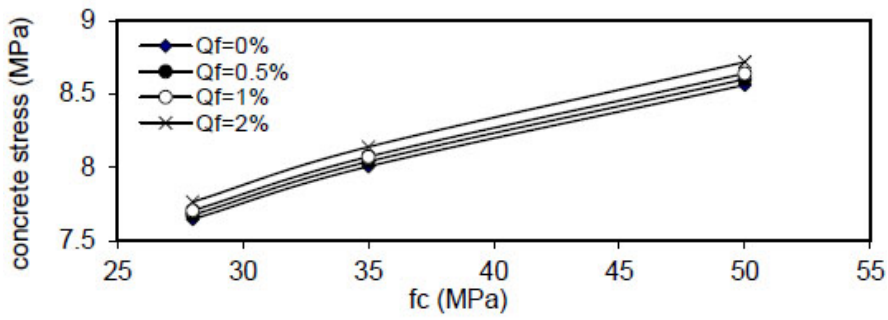


Fig. (29). Relation of f_c versus concrete stress ($\rho = 5\%$).

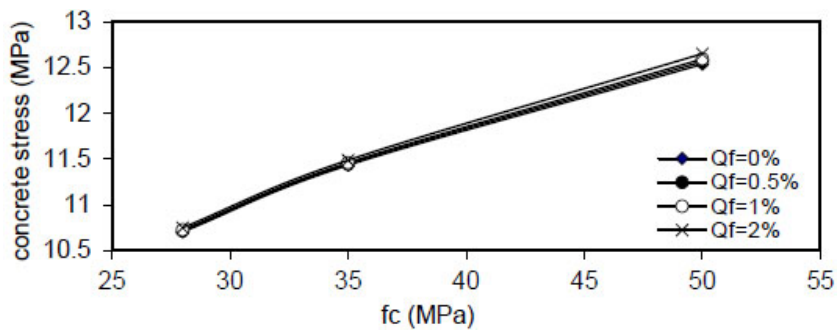


Fig. (30). Relation of f_c versus concrete stress ($\rho = 10\%$).

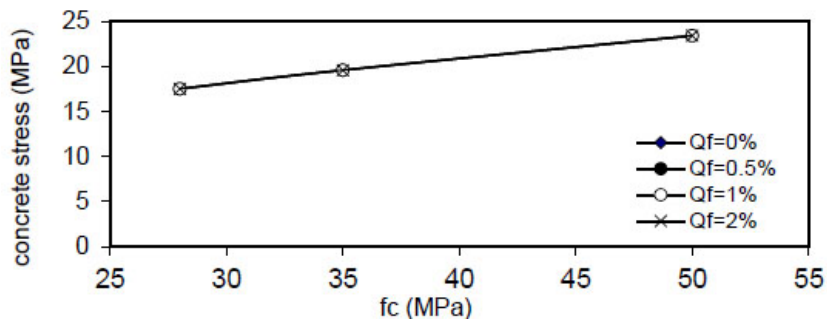


Fig. (31). Relation of f_c versus concrete stress ($\rho = \text{Infinity}$).

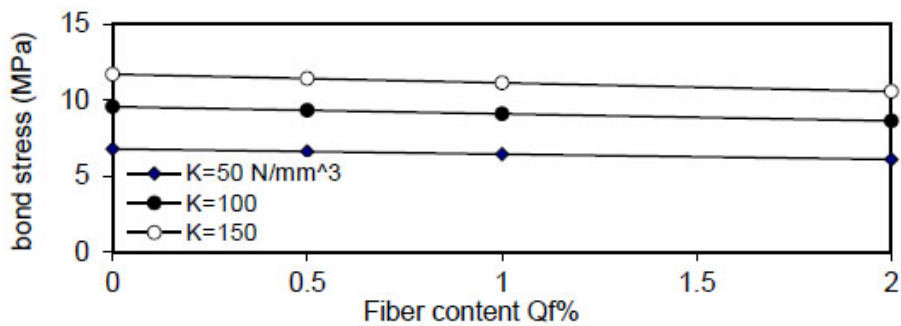


Fig. (32). Relation of Q_f versus concrete stress ($\rho = 1\%$).

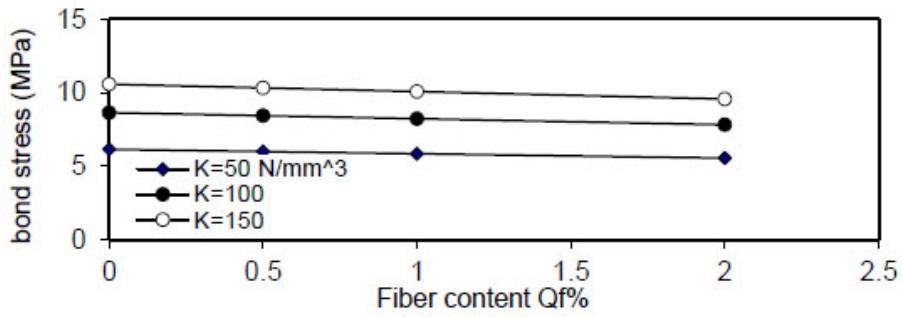


Fig. (33). Relation of Qf versus concrete stress (Rho=5%).

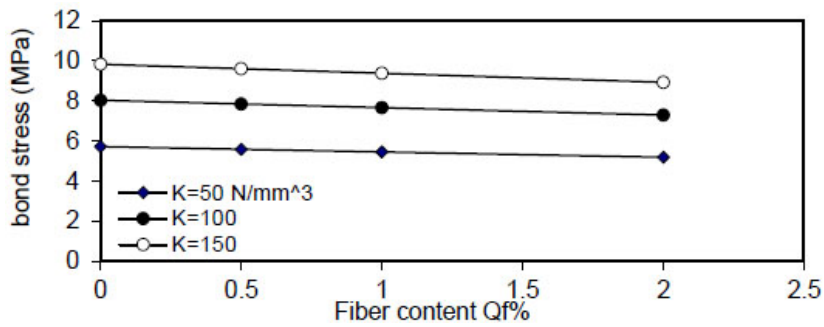


Fig. (34). Relation of Qf versus concrete stress (Rho=10%).

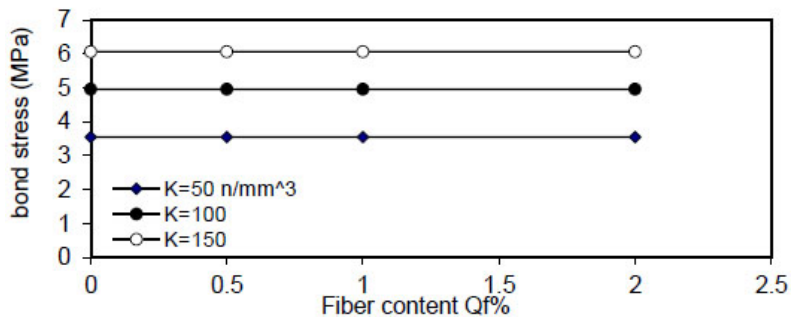


Fig. (35). Relation of Qf versus concrete stress (Rho=Infinity).

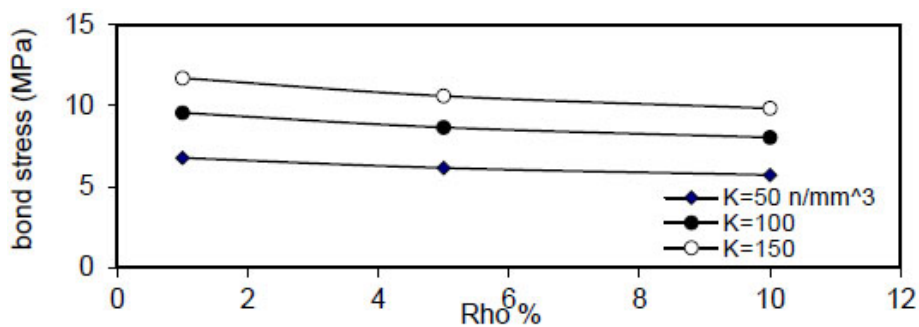


Fig. (36). Relation of (Rho %) versus concrete stress (Qf=0%).

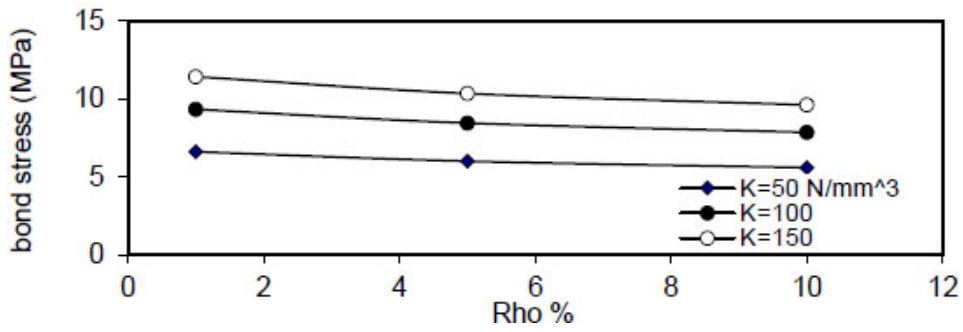


Fig. (37). Relation of (Rho %) versus concrete stress (Qf=0.5%).

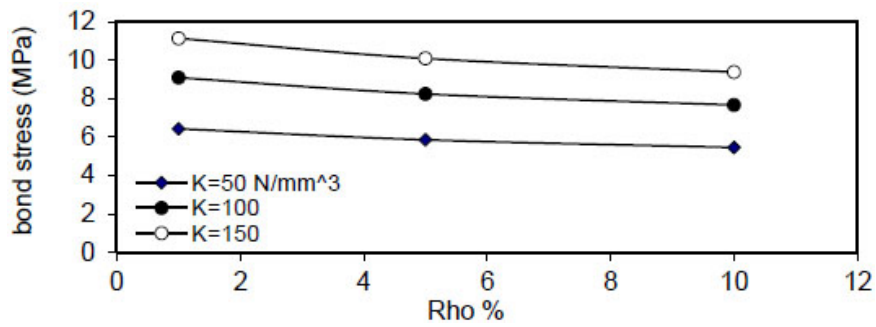


Fig. (38). Relation of (Rho %) versus concrete stress (Qf=1%).

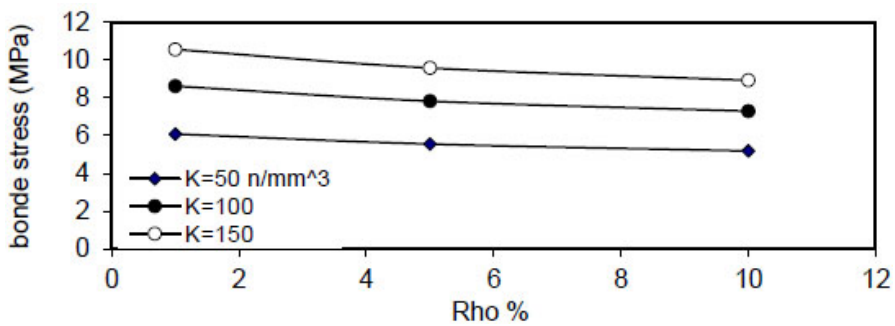


Fig. (39). Relation of (Rho %) versus concrete stress (Qf=2%).

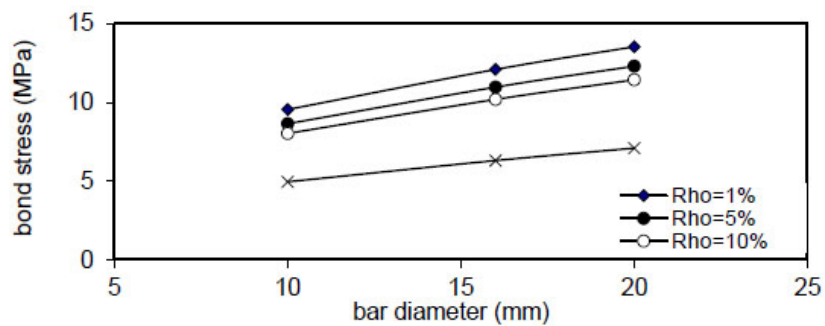


Fig. (40). Relation of bar diameter versus concrete stress (Qf=0%).

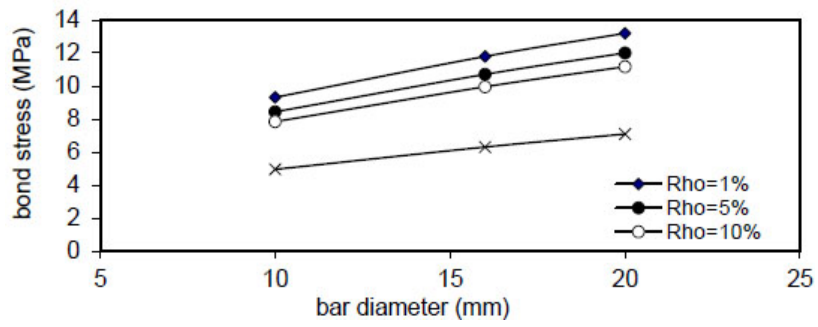


Fig. (41). Relation of bar diameter versus concrete stress ($Q_f=0.5\%$).

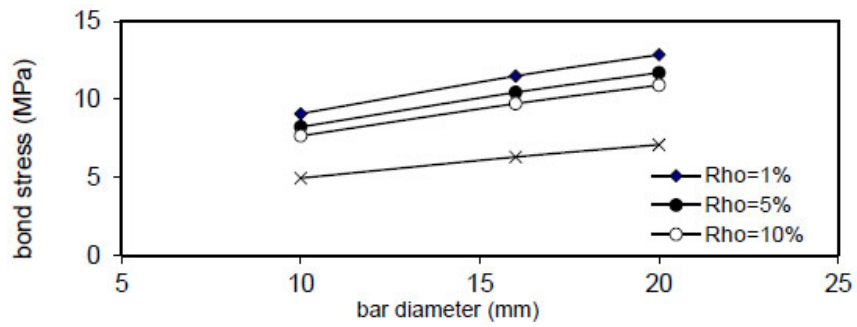


Fig. (42). Relation of bar diameter versus concrete stress ($Q_f=1\%$).

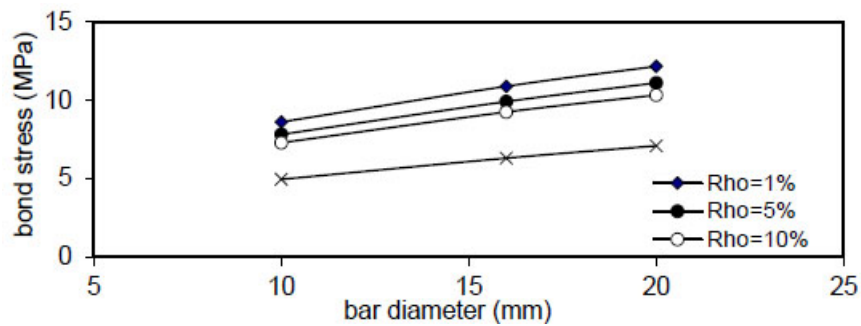


Fig. (43). Relation of bar diameter versus concrete stress ($Q_f=2\%$).

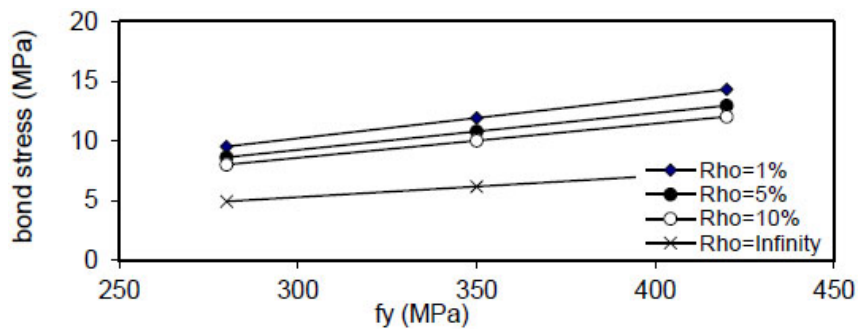


Fig. (44). Relation of f_y versus concrete stress ($Q_f=0\%$).

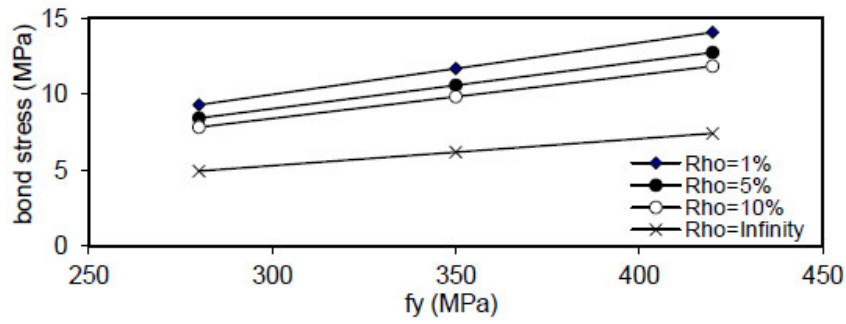


Fig. (45). Relation of f_y versus concrete stress ($Q_f=0.5\%$).

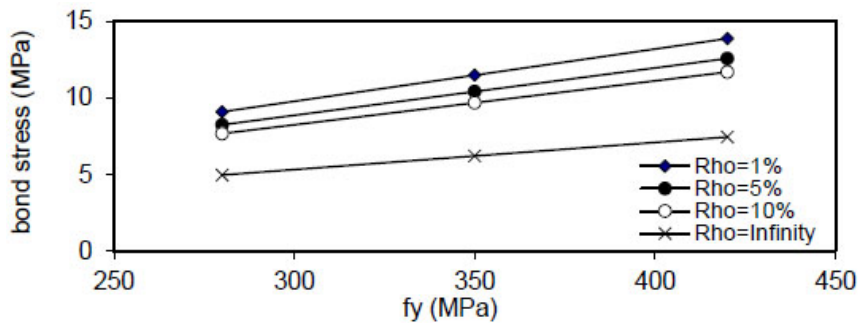


Fig. (46). Relation of f_y versus concrete stress ($Q_f=1\%$).

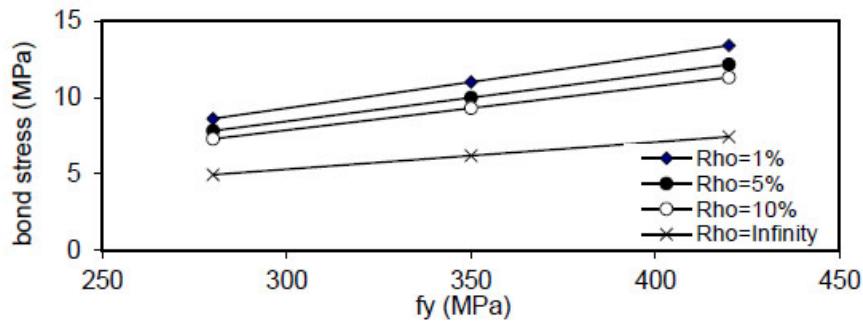


Fig. (47). Relation of f_y versus concrete stress ($Q_f=2\%$).

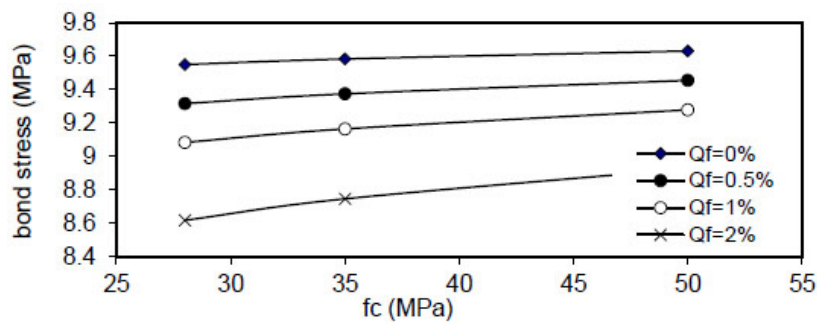


Fig. (48). Relation of f_c versus concrete stress ($Rho=1\%$).

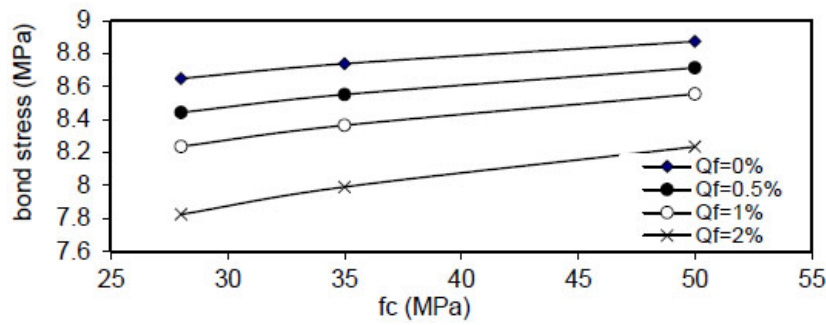


Fig. (49). Relation of f_c versus concrete stress (Rho=5%).

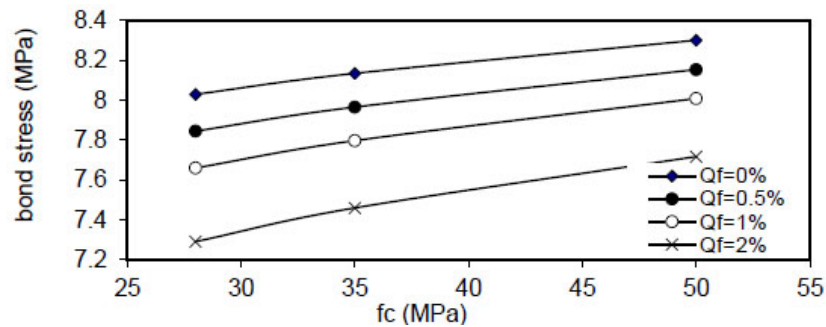


Fig. (50). Relation of f_c versus concrete stress (Rho=10%).

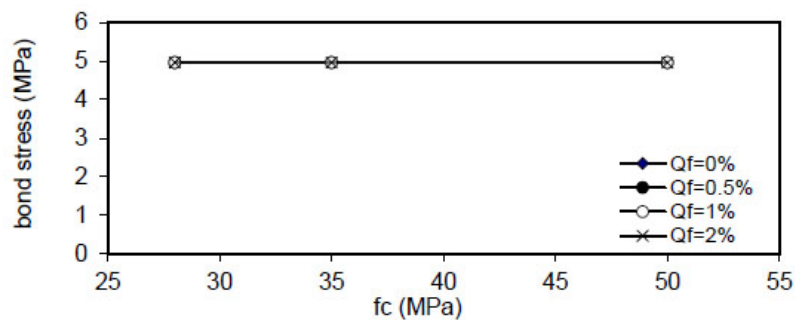


Fig. (51). Relation of f_c versus concrete stress (Rho=Infinity).

CONCLUSION

The results of the analysis show:

- 1) The variation of concrete stress (σ_c) along the length of the bar splice ($-\frac{L}{2}$ to $\frac{L}{2}$) for concrete without and with steel fiber ($Q_f=1\%$). The maximum stress is obtained at center $x=0$ and minimum at ($x = \pm \frac{L}{2}$).
- 2) The variation of bond stress (τ_1) between the steel bar and surrounding concrete for concrete without steel fiber and with steel fiber content ($Q_f=1\%$). The maximum value is obtained at ($x = \pm \frac{L}{2}$), and the minimum value at ($x = \frac{L}{2}$).
- 3) The variation of steel stress (σ_{s1}) in the splice bar

for both plain ($Q_f=0$) and fibrous concrete ($Q_f=1\%$). The maximum value is ($\sigma_{s1}=f_y$) at ($x = -\frac{L}{2}$) and the minimum value is ($\sigma_{s1}=0$) at ($x = \frac{L}{2}$). The value of τ_2 is the same as (τ_1) but in opposite sides, i.e., at ($\tau_2=\tau_1$). Also ($\sigma_{s2}=f_y$) at ($x = \frac{L}{2}$) and equal to zero at ($x = -\frac{L}{2}$).

4) The value of (σ_{cmax}) increased linearly with the increase of (ρ), the slope of the lines decreased with an increase of the value of displacement modulus (k) to ($100 \frac{N}{mm^3}$), the effect is negligible at ($k=150 N/mm^3$), the same behavior is noticed for ($\rho=5\&10\%$), but when ($\rho = \infty$), the effect of steel fiber content (Q_f) and steel bar reinforcement index ($\rho\%$) are neglected, and concrete stress becomes constant. The concrete stress increased nonlinearly (parabolic) with increasing of

($\rho\%$). Also, increasing value of (k) has a small effect on (σ_{cmax}). The same behavior is obtained for other steel fiber content.

5) The bar diameter has a negligible effect on maximum concrete stress for all steel fiber content (Q_f) and steel reinforcement content (ρ).

6) The maximum concrete stress (σ_{cmax}) increased linearly with (F_y) and concrete compressive strength (f'_c) and reduced when (ρ) increased from (1% to 5 & 10%) and became negligible at ($\rho=\infty$). This effect is increased when the value of (ρ) is increased, and the same behavior is noticed in fibrous concrete.

7) The relation of maximum bond stress (τ_{max}) and steel fiber content (Q_f) for ($\rho=1\%$), value of (τ_{max}) decreased linearly with increasing of (Q_f) for all values of (k) and (ρ) and decreased with increasing of ($\rho\%$) for all values of (Q_f & k). Also, using larger bar diameter (d_b) causes a linear increase in bond stress (τ_{max}). The value of (τ_{max}) increased with increasing of (f_y) for ($\rho=1,5,10\%$ and ∞) for plain concrete ($Q_f=0$) and fibrous concrete ($Q_f=0.5,1\&2\%$).

CONSENT FOR PUBLICATION

Not applicable.

AVAILABILITY OF DATA AND MATERIALS

Not applicable.

FUNDING

None.

CONFLICT OF INTEREST

The authors declare no conflict of interest, financial or otherwise.

ACKNOWLEDGEMENTS

Declared none.

REFERENCES

- [1] A. Losberg, "Anchorage of beam reinforcement shortened according to the moment distribution curve", *Seventh Congress of the IABSE, Final report, Rio de Janeiro*, pp. 383-392, 1964.
- [2] L.R. Felman, and F.M. Bartlett, "Bond stresses Along plain steel Reinforcing Bars in pullout specimens", *ACI-structural Journal*, vol. 104, no. 6, pp. 685-692, 2007.
- [3] M.K. Thompson, A. Ledesma, J.O. Jirsa, and J.E. Breen, "Lap splices anchored by headed bars", *ACI Struct. J.*, vol. 3, no. 2, pp. 271-279, 2006.
- [4] K.I. Coogler, K.A. Harries, and M. Gallick, "Experimental study of offset Mechanical Lap splice Behavior", *ACI Struct. J.*, vol. 105, no. 4, pp. 478-487, 2008.
- [5] L.R. Feldman, and F.M. Bartlett, "Bond in flexural Members with plain steel Reinforcement", *ACI Struct. J.*, vol. 105, no. 5, pp. 552-560, 2008.
- [6] K. Yang, and A.F. Ashour, "Mechanism analysis for concrete breakout capacity of single anchors in tension", *ACI Struct. J.*, vol. 105, no. 5, pp. 609-619, 2008.
- [7] H. Sezen, and E.J. Setzler, "Reinforcement slip in reinforced concrete columns", *ACI Struct. J.*, vol. 105, no. 3, pp. 280-289, 2008.
- [8] D.A. Howell, and C. Higgins, "Bond and development of deformed square reinforcing bars", *ACI Struct. J.*, vol. 104, no. 3, pp. 333-343, 2007.
- [9] R. Eligehausen, R.A. Cook, and J. Appl, "Behavior and design of adhesive bonded anchors", *ACI Struct. J.*, vol. 103, no. 6, pp. 822-831, 2006.
- [10] R. Tepfors, "Bond stress along lapped reinforcing bars", *Mag. Concr. Res.*, vol. 32, no. 112, pp. 135-142, 1980. [<http://dx.doi.org/10.1680/mac.1980.32.112.135>]
- [11] D.J. Hanant, *Fiber cements and fiber concretes.*, John Wiley and Sons Publication: New York, USA, 1978.
- [12] R.N. Swamy, R.S. Mangar, and K.C.U.S. Roa, *The mechanics of fiber reinforcement of cement materials*, ACI, SP-44, Detroit, 1974, pp. 1-28.
- [13] R. Narayanan, and A.S.K. Palanjian, "Effect of fiber addition on concrete strength", *Indian Concr. J.*, vol. 58, no. 4, pp. 100-103, 1984.
- [14] R. Narayanan, and A.S.K. Palanjian, "A space truss model for fiber concrete beams in torsion", *Struct. Eng.*, vol. 63B, no. 1, pp. 4-18, 1985.